

Spin configurations and negative coercivity in epitaxially grown DyFe₂/YFe₂ superlattices

S. N. Gordeev,^{a)} J.-M. L. Beaujour, G. J. Bowden, P. A. J. de Groot, and B. D. Rainford
*Department of Physics and Astronomy, University of Southampton, Southampton SO17 1BJ,
 United Kingdom*

R. C. C. Ward and M. R. Wells
Clarendon Laboratory, Oxford University, Oxford OX1 3PU, United Kingdom

Molecular beam epitaxial methods have been used to grow single crystal Laves phase DyFe₂/YFe₂ superlattice samples with a (110) growth direction. In particular, the magnetic properties of the YFe₂ dominated multilayer samples [*w*DyFe₂/*4w*YFe₂]*N* with *w* = 20, 30, 40, 45, 50, and 55 Å are presented and discussed. In principle, the multilayer films should possess similar magnetic properties because they are all nominally Dy_{0.2}Y_{0.8}Fe₂. However, it is shown that their magnetic properties depend strongly on the thickness of the DyFe₂ layers *w*. Those films with *w* ≥ 45 Å possess negative coercivities, while those with *w* ≤ 40 Å are positive. It is argued that this behavior can be understood in terms of a strong increase of the intrinsic coercivity of the DyFe₂/YFe₂ superlattice, taken as a whole, as *w* is reduced. For *w* ≤ 40 Å almost none of the DyFe₂ moments can be flipped over in the available field range (12 T). © 2001 American Institute of Physics.
 [DOI: 10.1063/1.1359465]

I. INTRODUCTION

Epitaxial multilayer films of DyFe₂/YFe₂ can be grown with specific magnetic properties. For example, films have been produced with magnetic compensation points,¹ tailored coercive fields,² model magnetic exchange springs that scale closely with 1/*w*², where *w* is the thickness of the magnetically soft YFe₂ layers,³ and negative coercivities.^{4,5} Such films should find applications in magnetostrictive and spintronic devices.^{6,7} In general, the properties of DyFe₂/YFe₂ superlattices are characterized by (i) a dominant ferromagnetic Fe–Fe exchange (~600 T), (ii) a weaker antiferromagnetic Dy–Fe exchange (~100 T), and (iii) a Dy crystal field anisotropy (~10–100 T). The latter determines the direction of easy magnetization, which is [001] at temperatures below 100 K.^{8,9} Consequently, in zero field and at low temperatures, the net moments of the DyFe₂ (~7 μB per formula unit) and YFe₂ (~3 μB) are aligned antiferromagnetically along a [001] axis. Since the thickness of the YFe₂ layers is four times that of the DyFe₂ layers, the net magnetic moment is YFe₂ dominated.

In the presence of an applied field, magnetic exchange springs, set up within the YFe₂ layers, play an important role in determining the magnetization of the superlattice.^{3–5,10} Such springs are characterized by a critical bending field *B_B*.^{3–5,10–14} For fields less than *B_B*, all the Fe magnetic moments in both YFe₂ and DyFe₂ layers are aligned parallel to each other due to the strong Fe–Fe magnetic exchange. But when the applied field exceeds *B_B*, it becomes energetically favorable for the magnetic moments within the soft YFe₂ layers to rotate, forming exchange springs, pinned at the edges by the neighboring hard DyFe₂ layers. Conversely, when the field is removed, the magnetic exchange springs

unwind giving rise to a net negative magnetic moment, even though the applied field is still positive.^{4,5}

In this article the problem of designing films with negative coercivities is examined in more detail. In all, results are collated and discussed for six YFe₂ dominated multilayer samples [*w*DyFe₂/*4w*YFe₂]*N* where *w* = 20, 30, 40, 45, 50, and 55 Å. Nominally, all these samples should possess the same magnetic properties. However, it is shown that the sign of the coercivity of the superlattices changes from negative to positive with decreasing thickness *w*.

II. EXPERIMENT

The (110) Laves phase DyFe₂/YFe₂ superlattices in this work were grown by molecular beam epitaxial methods, as described elsewhere.^{1,15} The samples were deposited on epiprepared (11 $\bar{2}$ 0) sapphire substrates with a 500 Å (110) Nb buffer and a 30 Å seed layer of Fe. All the samples were YFe₂ dominated, in the sense that the magnetic moment of the YFe₂ component exceeded that of the DyFe₂. The magnetic measurements were made using a 12 T vibrating sample magnetometer.

III. RESULTS AND DISCUSSION

The magnetization curve, for the sample *w* = 45 Å, can be seen in Fig. 1. This data was obtained at 10 K for fields applied along the easy [001] axis. For convenience the magnetization *M* has been converted to Bohr magnetons per average formula unit (Dy_{0.2}Y_{0.8}Fe₂). For the three multilayer films, with *w* = 45, 50, and 55 Å, the measured coercivity is negative. However, This is not the case for the films with *w* = 20, 30, and 40 Å. Magnetization curves for *w* = 30 and 40 Å can be seen in Fig. 2. It will be observed that the

^{a)}Electronic mail: sg@phys.soton.ac.uk

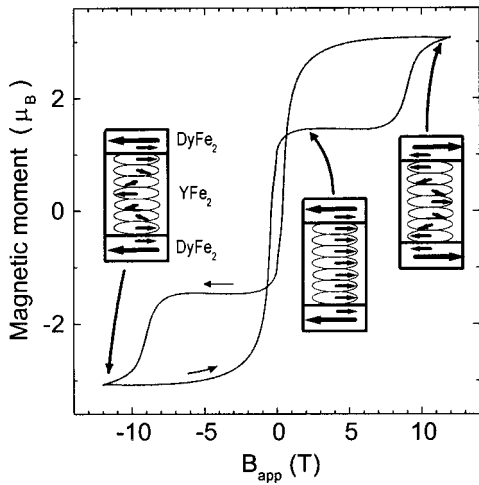


FIG. 1. In-plane [001] magnetization curve for the superlattice film $[w\text{DyFe}_2/4w\text{YFe}_2] \times N$ for $w=55 \text{ \AA}$ and $N=15$ at $T=10 \text{ K}$. Insets show spin configurations. Bold (thin) arrows represent Dy (Fe) moments, respectively.

coercivity is positive and close to zero. The measured coercivities for the six superlattices investigated are summarized in Fig. 3.

An interpretation of the magnetization curve with negative coercivity has already been given in Ref. 5. In a large negative applied field $B_{\text{app}}(-12 \text{ T})$, the minimum energy state is achieved with the net moment of the DyFe_2 layers ($\sim 7\mu_B$) all pointing along B_{app} , with magnetic exchange springs set up in the thicker YFe_2 layers (see insets to Fig. 1). However, as the strength of the applied field is reduced, the YFe_2 exchange springs unwind until the applied field reaches the critical bending field $B_B(\sim 1 \text{ T})$. For a symmetric ex-

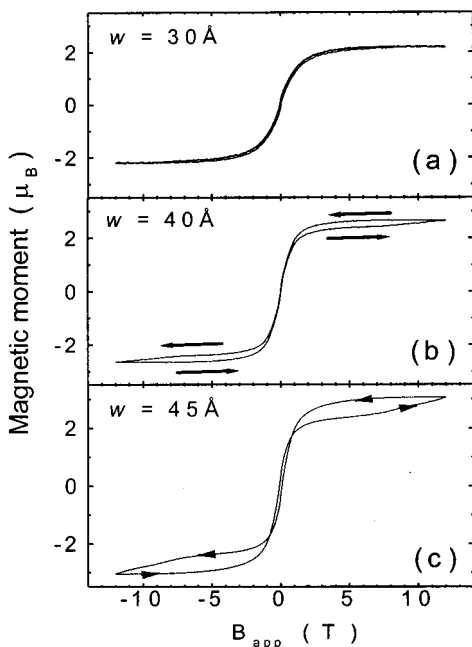


FIG. 2. In-plane [001] magnetization curves for the superlattice films $[w\text{DyFe}_2/4w\text{YFe}_2] \times N$ for $w=30, 40,$ and 45 \AA , and $N=27, 20,$ and 18 , respectively, at $T=10 \text{ K}$.

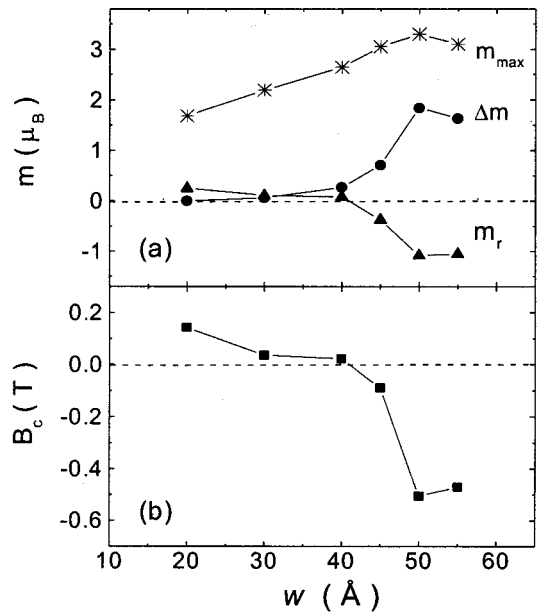


FIG. 3. The remanent magnetic moment m_r , the magnetization step at $B_{\text{irr}}, \Delta m$, and the magnetic moment at $B_{\text{app}}=12 \text{ T}, m_{\text{max}}$ (a), and the coercive field B_c (b) for six $[w\text{DyFe}_2/4w\text{YFe}_2] \times N$ samples at 10 K .

change spring this bending field is given by $B_B = B_{\text{ex}}(\pi/n)^2$, where B_{ex} is the exchange field and n is the number of monolayers in the spring.¹⁴ When the applied field falls below this value the exchange spring becomes unstable with the creation of the antiferromagnetic state. Since all our samples are YFe_2 dominated, this state is characterized by a positive magnetic moment $\sim 1.0\mu_B$ per formula unit. The magnetization is positive even though the applied field is still negative. On increasing the magnetic field still further, the magnetic moment stays constant, at $\sim 1.0\mu_B$, until $B_{\text{app}} = B_{\text{irr}} \sim 7.5 \text{ T}$. Indeed, if this field is not exceeded, the magnetization curve between -12 T and B_{irr} is completely reversible, a classic signature of magnetic exchange spring behavior. However, when B_{irr} is exceeded, the system becomes unstable with irreversible flips in the magnetic moments of the DyFe_2 layers, accompanied by the simultaneous creation of magnetic exchange springs in the YFe_2 layers.^{4,5} Finally, when all the DyFe_2 layers have been flipped over, we arrive at the spin configuration shown in the inset of Fig. 1 for $B_{\text{app}}=12 \text{ T}$.

The magnetization curves obtained at $T=10 \text{ K}$ for the three samples $w=30, 40,$ and 45 \AA can be seen in Fig. 2. Here the measured coercivities B_c and the remanent magnetic moments m_r are almost zero. All the curves are practically reversible. Note also that the step (Δm) in the magnetization, associated with flipping the DyFe_2 layers at B_{irr} , vanishes when $w \leq 30 \text{ \AA}$. The step Δm , the coercivity B_c , the remanent moments m_r , and the maximum magnetic moment m_{max} , as a function of w , are all summarized in Fig. 3.

The apparent differences between the magnetization curves of Figs. 1 and 2 can be understood as follows. First we observe, from an examination of Fig. 3, that the switching of the DyFe_2 layers, as indicated by the step Δm , is effectively suppressed when w falls below 40 \AA . Second, there is a concomitant fall in the maximum magnetic mo-

ment $m_{\max}(3.2 \rightarrow 1.7 \mu_B)$ as w is decreased. The latter suggests therefore that the contribution to overall magnetic moment by the DyFe₂ layers is missing when $w \leq 40 \text{ \AA}$. In addition, in these samples the ruminant magnetic moment is very small, despite being cycled in a field of 12 T. Thus the DyFe₂ layers must be frozen, in an antiferromagnetic domain pattern, and cannot be aligned even in a field of 12 T.

We can understand why this behavior occurs in terms of the energy changes associated with switching of the DyFe₂ layers. In the first place, there will be a gain in the Zeeman energy associated with the switching of the DyFe₂ layers themselves. However, this gain comes at a penalty. When the DyFe₂ layers are switched, exchange springs are necessarily set up in the YFe₂ layers. This results in two energy losses that can offset the gain in the YFe₂ Zeeman energy. One, a loss in Fe–Fe exchange energy, because the Fe moments are no longer parallel to each other. Two, a loss in YFe₂ Zeeman energy, which we estimate to be $\sim 2.4[\langle \cos \theta \rangle - 1] \mu_B$ per formula unit, where $\langle \cos \theta \rangle$ is the average projection of the exchange spring moments in the direction of the applied field.¹⁴ In practice, $\langle \cos \theta \rangle$ increases with increasing the thickness of the YFe₂ and/or increasing the strength of the applied field. Thus the field B_{irr} , at which the switching of the DyFe₂ layers becomes energetically favorable, shifts to higher B_{app} when w decreases. Ultimately therefore, switching of the DyFe₂ layers will be suppressed if there is insufficient energy (magnetic field) to drive the transition.

Finally, we offer the following interpretation for the multilayer film with $w = 30 \text{ \AA}$. Here almost none of the DyFe₂ layers can be flipped over in a field of 12 T. So the DyFe₂ layers are presumably trapped in an antiferromagnetic state, with zero net magnetic moment. However, as the magnetic field is increased, magnetic exchange springs form in the soft YFe₂ layers. Such springs will give rise to reversible magnetization and an almost vanishing hysteresis loop, as observed.

IV. CONCLUSIONS

We have performed magnetization studies of $[w\text{DyFe}_2/4w\text{YFe}_2] \times N$ superlattices with $w = 20\text{--}55 \text{ \AA}$. It was found that while magnetic properties of all these sample are largely determined by the formation of exchange springs, the coercive field B_c and the ruminant field m_r are strongly dependent on the thickness w . For $w \geq 45 \text{ \AA}$ the superlattices

show $B_c < 0$ and $m_r < 0$. Whereas for $w \leq 40 \text{ \AA}$, both B_c and m_r are positive and the magnetization curves are practically reversible. We attribute these changes to an increase in the B_{irr} of the superlattice as a whole, as the thickness w is decreased. In particular, for $w \leq 40 \text{ \AA}$ flipping of the DyFe₂ layers is effectively suppressed by the energy requirements associated with the setting up of exchange springs in the YFe₂ layers. In such samples, the DyFe₂ moments are frozen in an antiferromagnetic state and make little or no contribution to the net magnetic moment. Thus the magnetization loop is almost entirely determined by the magnetic exchange springs, in the soft YFe₂ layers.

ACKNOWLEDGMENTS

This work has been supported by the UK Engineering and Physical Sciences Research Council and by Technology Group 4 (Materials and Structures) of the MoD Corporate Research Program.

- ¹M. Sawicki, G. J. Bowden, P. A. J. de Groot, B. D. Rainford, R. C. C. Ward, and M. R. Wells, *J. Appl. Phys.* **87**, 6839 (2000).
- ²M. Sawicki, G. J. Bowden, P. A. J. de Groot, B. D. Rainford, J.-M. L. Beaujour, R. C. C. Ward, and M. R. Wells, *Appl. Phys. Lett.* **77**, 573 (2000).
- ³M. Sawicki, G. J. Bowden, P. A. J. de Groot, B. D. Rainford, R. C. C. Ward, and M. R. Wells, *Phys. Rev. B* **62**, 5817 (2000).
- ⁴J.-M. L. Beaujour, G. J. Bowden, S. Gordeev, P. A. J. de Groot, B. D. Rainford, R. C. Wells, and M. R. Wells, *J. Magn. Magn. Mater.* (to be published).
- ⁵J.-M. L. Beaujour, G. J. Bowden, S. Gordeev, P. A. J. de Groot, and B. D. Rainford, *Appl. Phys. Lett.* **78**, 964 (2001).
- ⁶A. E. Clark, M. Wun-Fogle, J. P. Teter, J. B. Restorff, and S. F. Cheng, *J. Appl. Phys.* **76**, 7009 (1994).
- ⁷A. Barthélémy, A. Fert, and F. Petroff, in *Handbook of Magnetic Materials*, edited by K. H. J. Buschow (Elsevier, Amsterdam, 1999), Vol. 12, Chap. 1.
- ⁸K. H. J. Buschow, *Rep. Prog. Phys.* **40**, 1179 (1977).
- ⁹J. J. M. Franse and R. J. Radwanski, in *Handbook of Magnetic Materials*, edited by K. H. J. Buschow (North Holland, Amsterdam, 1993), Vol. 7.
- ¹⁰K. Dumesnil, M. Dutheil, C. Dufour, and Ph. Mangin, *Phys. Rev. B* **62**, 1136 (2000).
- ¹¹E. Goto, N. Hayashi, T. Miyashita, and K. Nakagawa, *J. Appl. Phys.* **36**, 2951 (1965).
- ¹²E. E. Fullerton, J. S. Jiang, M. Grimsditch, C. H. Sowers, and S. D. Bader, *Phys. Rev. B* **58**, 12193 (1998).
- ¹³E. E. Fullerton, J. S. Jiang, and S. D. Bader, *J. Magn. Magn. Mater.* **200**, 392 (1999).
- ¹⁴G. J. Bowden, J.-M. L. Beaujour, S. Gordeev, P. A. J. de Groot, B. D. Rainford, and M. Sawicki, *J. Phys.: Condens. Matter* **12**, 9335 (2000).
- ¹⁵V. Odero, C. Dufour, K. Dumesnil, Ph. Bauer, Ph. Mangin, and G. Marcal, *Phys. Rev. B* **54**, R17375 (1996).